microplastics

MDPI

Article

Cytotoxic Potential of Environmentally Relevant PVC Micro- and Nanoplastics of Varied Size, Shape, and Surface Degradation

Phyo Bo Bo Aung [1], Yuya Haga [1,2,*], Sota Manabe [2], Wakaba Idehara [2], Mii Hokaku [1,2], Yuto Motoyama [1], Ayaha Mori [2], Kazuma Higashisaka [1,2,3] and Yasuo Tsutsumi [1,2,4,5,6,7,*]

1 Graduate School of Pharmaceutical Sciences, The University of Osaka, 1-6 Yamadaoka, Suita, Osaka 565-0871, Japan
2 School of Pharmaceutical Sciences, The University of Osaka, 1-6 Yamadaoka, Suita, Osaka 565-0871, Japan
3 Institute for Advanced Co-Creation Studies, The University of Osaka, 1-6 Yamadaoka, Suita, Osaka 565-0871, Japan
4 Graduate School of Medicine, The University of Osaka, 2-2 Yamadaoka, Suita, Osaka 565-0871, Japan
5 Institute for Open and Transdisciplinary Research Initiatives, The University of Osaka, 1-1 Yamadaoka, Suita, Osaka 565-0871, Japan
6 Global Center for Medical Engineering and Informatics, The University of Osaka, 2-2 Yamadaoka, Suita, Osaka 565-0871, Japan
7 R3 Institute for Newly-Emerging Science Design, The University of Osaka, 1-3 Machikaneyamacho, Toyonaka, Osaka 560-8531, Japan
* Correspondence: haga-y@phs.osaka-u.ac.jp (Y.H.); ytsutsumi@phs.osaka-u.ac.jp (Y.T.)

Abstract

Microplastics (MPs), i.e., plastic particles <5 mm, and nanoplastics (NPs), i.e., plastic particles <1 μm, are widespread in the environment. MPs and NPs (MNPs) have also been detected in human tissues. Environmental MNPs exhibit diverse physicochemical properties such as size, shape, and surface degradation. However, most experimental studies have used pristine MNPs, which poorly represent real-world conditions, and only a limited number of studies have focused on preparing environmentally relevant MNPs. Therefore, we focused on the key physicochemical properties of MNPs, particularly their shape, size, and surface degradation, using polyvinyl chloride (PVC) as the model polymer. In this study, fragment and spherical PVC-MNPs were utilized, and surface degradation was introduced through exposure to vacuum ultraviolet (VUV) radiation at a wavelength of 172 nm. Attenuated Total Reflectance-Fourier Transform Infrared (ATR-FTIR) analysis revealed the formation of additional carbonyl groups after VUV exposure. We investigated the cytotoxic effects of the degraded and non-degraded PVC-MNPs on A549, Caco-2, and THP-1 cells. The results indicated that the degraded PVC-MNP-treated groups induced higher cytotoxic effects than those in the non-degraded groups. Notably, the degraded PVC-NPs induced stronger cytotoxicity than the degraded PVC-MPs. These findings highlight the potential health risks associated with environmental MNPs.

Keywords: microplastics; nanoplastics; polyvinyl chloride; vacuum ultraviolet (VUV); degradation; cytotoxicity

Received: 20 February 2026
Revised: 19 March 2026
Accepted: 14 April 2026
Published: 1 May 2026

1. Introduction

In the 21st century, plastic pollution has become one of the most pressing environmental challenges owing to the increasing global population and economy, which leads to increased plastic consumption and plastic products [1,2]. In 2019, the annual worldwide

output of plastic products reached 460 million tons [1]. Moreover, Organisation for Economic Co-operation and Development (OECD) has suggested that plastic waste could triple by 2060 [3]. This has emerged as a critical global concern because it causes a wide range of damage to ecosystems and human health. Microplastics (MPs) are plastic particles with diameters less than 5 mm and a major component of plastic waste. These particles are now ubiquitous in the environment [1,4]. They are classified into two types: primary MPs, which are intentionally manufactured and directly released into the environment, and secondary MPs, which result from the degradation of larger plastic objects over time [5,6]. When MPs undergo physical breakdown, they form smaller particles. Similarly, nanoplastics (NPs), plastic particles with a diameter of less than 1 μm, are widespread in the environment and pose additional challenges owing to their small size and potential for cellular uptake [7]. MPs and NPs (MNPs) have been observed in all components of the environment, including the ocean, soil, air [8], and many human consumer products [8,9]. Humans are estimated to be exposed to thousands to millions of MNPs annually or several milligrams daily via three major pathways: inhalation, ingestion, and skin contact [1,10]. Consequently, MNPs have been found in selected human tissues, such as the liver, kidney, brain [11], heart [12,13], and placenta [14], and fluids, such as breast milk [15], urine [16], and blood [16]. The presence of MNPs in humans has been reported to be associated with serious health issues, including cardiovascular diseases [12], inflammatory bowel diseases [17], respiratory and neurological disorders, and various cancers [18]. One of the first studies to directly examine the risks of microplastic exposure in humans reported that patients with carotid artery plaques in which MNPs were detected had a higher risk of heart attack, stroke, and death than those without [19].

Furthermore, MNPs present in the environment are highly heterogeneous, not only in terms of polymer type but also in size, shape, and surface properties [20,21]. However, most experimental studies evaluating the health risks of MNPs have relied on pristine and spherical polystyrene (PS) beads, which do not adequately reflect the complex physicochemical characteristics of environmental samples, although irregular, surface-oxidized fragment dominate real environmental MNPs [22]. Bridging this gap requires the development of more representative MNP materials that reflect the complexity and surface oxidation observed under real-world conditions. Environmental stressors such as ultraviolet (UV) radiation exposure can cause surface oxidation of MNPs [23–25]. To address this issue, we developed a platform to prepare MNPs with surface-degraded samples that mimic environmentally weathered surfaces [24,26]. Previous studies have demonstrated that surface-degraded MNPs can significantly influence cellular responses compared to non-degraded MNPs [26–28], highlighting the importance of considering their physicochemical properties, particularly on surface degradation. Polymer type is another critical variable. However, most studies on MNP toxicity have utilized PS and polyethylene (PE) MNPs because of their commercial availability and widespread production. In contrast, polyvinyl chloride (PVC) has received limited attention in MNP research, although it is the third most widely produced and environmentally persistent polymer [22] and has been detected in human tissues [11,19]. To date, only a limited number of studies have focused on preparing environmentally relevant PVC-MNPs. In response, this study aimed to develop MNP samples by considering key physicochemical properties, particularly size, shape, and surface degradation, and evaluating their cytotoxicity across different cell lines, with the goal of providing foundational data for hazard assessment.

2. Materials and Methods

2.1. PVC-MP Samples

PVC powder with a particle size of (117 ± 17) μm was purchased from FUJIFILM Wako Pure Chemical Corporation (Osaka, Japan) and used as PVC-MP samples.

2.2. Preparation of Spherical PVC-NPs

Spherical PVC-NPs were prepared following a previously reported method [29] and using PVC-MP powder (FUJIFILM Wako Pure Chemical Corporation, Osaka, Japan). Twelve milligrams of the PVC-MPs were weighed and placed in a glass test tube. Then, the sample was dissolved in 3 mL of cyclohexanone (FUJIFILM Wako Pure Chemical Corporation, Osaka, Japan) and heated at 60 °C for at least 3 h until completely dissolved. For precipitation, 100 mL of antisolvent mixture of distilled water and dimethyl sulfoxide (DMSO) (FUJIFILM Wako Pure Chemical Corporation, Osaka, Japan) (35:65, *v/v*) was prepared in a heat-resistant glass bottle equipped with a magnetic stirrer and maintained at 40–42 °C. The polymer solution (3 mL) was added to the antisolvent at a constant rate using a glass syringe. After addition, the mixture was cooled by immersion in room-temperature water. Once cooled, the solution was filtered through a stainless-steel mesh filter (pore size: 0.2 mm) to remove large aggregates. Vacuum filtration (WJ-20; SIBATA, Saitama, Japan) was performed using a polyester track-etched membrane filter with a 1 μm pore size (GVS, Bologna, Italy). As NP particles tended to aggregate on the surface of the 1 μm filter, ethanol was used as an organic antisolvent to suspend the particles, aided by sonication with a Handy Sonic UH-50 (SMT Co., Ltd., Tokyo, Japan). Subsequently, filtration was repeated using a 0.2 μm (GVS, Bologna, Italy) membrane filter to collect NP particles smaller than 1 μm. The NP particles retained on the 0.2 μm filter were dispersed in t-butyl alcohol (Nacalai Tesque, Kyoto, Japan) and freeze-dried using a UT-1010 lyophilizer (EYELA, Tokyo, Japan). Additive-free PVC was used as the starting material to ensure the chemical integrity of NP particles throughout the preparation process. After each preparation, the collected particles were routinely analyzed using Attenuated Total Reflectance-Fourier Transform Infrared (ATR-FTIR) spectroscopy for quality control.

2.3. Preparation of Fragment PVC-NPs

Fragment PVC-NPs were prepared by modifying the protocol described by WS Lee et al., 2022 [30]. Then, 100 mg of PVC-MPs were weighed and placed in a 100 mL glass bottle. The sample was dissolved and incubated in 10 mL of cyclohexanone under magnetic stirring at 1000 rpm and heated at 60 °C for 30 min. After incubation, the polymer solution was cooled to 25 °C, and 80 mL of 99.5% ethanol (Nacalai Tesque, Kyoto, Japan) was added at a constant rate. The resulting mixture was filtered by vacuum filtration using a polyester track-etched membrane filter with a pore size of 0.2 μm (GVS, Bologna, Italy). The particles retained on the 0.2-μm filter were dispersed in t-butyl alcohol and freeze-dried using a UT-1010 lyophilizer. The collected NP particles were analyzed by ATR-FTIR to confirm their chemical integrity, using the same procedure as in the preparation of the spherical PVC-NPs.

2.4. MNP Degradation

The degradation of the PVC-MNPs was conducted following previously established protocols and was performed using a FLAT EXCIMER EX-mini system (Hamamatsu Photonics K. K., Shizuoka, Japan), which emitted vacuum ultraviolet (VUV) light at a wavelength of 172 nm with an intensity of 50 mW/cm^2 over an irradiation area of 86 × 40 mm. The PVC powder was evenly spread on the bottom of a Petri dish, placed approximately

10 mm from the light source, and irradiated with VUV light. After the VUV treatment, the degraded PVC-MNP samples were collected in a sample bottle.

2.5. ATR-FTIR Measurement

To confirm PVC-MNP degradation, an ATR-FTIR spectrometer was used with an FT/IR-4700 spectrophotometer (Jasco, Tokyo, Japan) equipped with a TGS detector. A diamond ATR crystal (incident angle: 45°, approximately one reflection) mounted on a horizontal ATR accessory was used for sample analysis. Spectra were acquired between 4000 and 400 cm^{-1}. To measure the IR spectra of the PVC-MNPs, a background spectrum was first recorded and the PVC-MNP samples were subsequently measured. The raw spectra were presented as ATR-FTIR spectra, calculated as $-\log(I/I_0)$, where I is the sample spectral intensity and I_0 is the background intensity measured prior to sample acquisition.

2.6. Carbonyl Index (CI)

The carbonyl index (CI) was determined by evaluating the ratio of the peak heights corresponding to the C=O stretching band at 1726 cm^{-1} and C-H band at 1426 cm^{-1}. The ATR-FTIR spectra of PVC-MNPs before and after exposure to VUV irradiation revealed distinct changes in the chemical structure. Following VUV treatment, a new peak corresponding to the C=O stretching band emerged at 1726 cm^{-1}, indicating the formation of carbonyl groups and confirming surface oxidation of the polymer.

This analytical approach has been previously validated by comparing the CI values of VUV-treated PE with those of environmentally weathered PE-MPs as reported by Ikuno et al. [24] demonstrating comparable levels of oxidative degradation.

2.7. Microscopic Imaging

The PVC-MP samples were transferred to dedicated 96-well plates and imaged using a CellVoyager 8000 high-content screening system (Yokogawa Inc., Tokyo, Japan).

2.8. Scanning Electron Microscopy (SEM) Imaging

Scanning electron microscopy (SEM) was performed using field-emission SEM. Prior to SEM analysis, 0.5 mg of PVC-NP samples were dispersed in 100 µL ethanol and sonicated for over 30 min to ensure uniform suspension. After sonication, 1 µL of PVC-NP solution was loaded onto silicon wafer chips, and vacuum-dried at room temperature. Subsequently, the PVC-NPs were coated with osmium (Neoc CS; Meiwafosis Co., Ltd., Tokyo, Japan). The osmium-coated PVC-NP samples were then placed onto carbon adhesive tape and imaged at an acceleration voltage of 3.0 kV using a S-4800 high-resolution SEM (Hitachi High-Tech, Tokyo, Japan).

2.9. Size and Shape Analysis

Microscopic and SEM images of 30 individual PVC-MNP particles were acquired and analyzed for morphological characterization using the ImageJ software (version 2.14.0/1.54f), where the maximum Feret diameter and roundness of each particle were quantified. In this analysis, roundness was calculated using the equation: $4 \times \text{area}/(\pi \times \text{diameter}^2)$. A value of 1 represents a perfect circle with roundness ranging from 0 to 1.

2.10. Cell Culture

Human alveolar adenocarcinoma (A549), human intestinal epithelial (Caco-2), and human monocytic leukemia (THP-1) cells were used in this study. A549 cells were cultured in Dulbecco's Modified Eagle Medium (high glucose) supplemented with L-glutamine and phenol red (FUJIFILM Wako Pure Chemical Corporation, Osaka, Japan), 10% fetal bovine serum (FBS; Biosera, Nuaille, France), and a 1% (*v/v*) penicillin-streptomycin-amphotericin

B suspension (Antibiotics; Ab) (FUJIFILM Wako Pure Chemical Corporation, Osaka, Japan). Caco-2 cells were cultured in Eagle's Minimum Essential Medium (FUJIFILM Wako Pure Chemical Corporation, Osaka, Japan) supplemented with 10% FBS and 1% Ab. THP-1 cells were maintained in an RPMI-1640 medium (FUJIFILM Wako Pure Chemical Corporation, Osaka, Japan) containing 10% FBS, 1% Ab, and 0.1% 2-mercaptoethanol (Thermo Fisher Scientific, Waltham, MA, USA). Cultures were maintained at 37 °C in a humidified incubator with 5% CO_2 and >95% relative humidity.

2.11. Cell Viability Assay

Cell viability was assessed using the 3-(4,5-dimethylthiazol-2-yl)-2,5-diphenyl tetrazolium bromide (MTT) assay (Tokyo Chemical Industry, Tokyo, Japan) following the manufacturer protocol. Cells were incubated with MNP samples suspended in culture medium containing 0.1% carboxymethyl cellulose (CMC) to improve particle dispersion for 24 h before the addition of the MTT reagent. To avoid interference with the MTT assay, after incubation with the MTT reagent for 3 h, all reagents, including MNP samples and the MTT reagent, were removed by inverting the 96-well plate, leaving only the MTT-reacted cells attached to the wells prior to absorbance measurement.

2.12. Statistical Analysis

The inhibitory concentration (IC_{50}) values for cell viability were calculated using GraphPad Prism 10 for MacOS (version 10.6.0). Data are presented as mean values ± standard deviation. For MTT assay, significance was assessed using two-way ANOVA followed by Bonferroni's multiple comparisons test. Statistical significance was considered at $p < 0.05$.

3. Results

3.1. Physicochemical Characterization of PVC-MNPs

In this study, fragment PVC-MPs were used as larger particles, and spherical and fragment PVC-NPs were successfully synthesized using a precipitation-based method (Figure 1A) and used as smaller NP samples. The shape and size of the particles were analyzed based on roundness and Feret diameter measurements using microscopic and SEM images. Roundness, a measure of the circularity of a particle, ranged from 0 to 1, with values closer to 1 indicating particles approaching a perfect circle. The roundness of fragment PVC-MPs was (0.75 ± 0.10), whereas spherical PVC-NPs exhibited a higher roundness of (0.93 ± 0.06). The fragmented PVC-NPs exhibited a roundness of (0.54 ± 0.16) (Figure 1B). Feret diameter measurements revealed that the diameter of the fragment PVC-MPs was (117 ± 17) µm, whereas the spherical and fragment PVC-NPs had diameters of (306 ± 122) and (225 ± 92) nm, respectively (Figure 1C). The surface impurities of each plastic particle were further examined using ATR-FTIR (Figure 1D), and no additional peaks were observed in the PVC spectra.

3.2. Correlation Analysis of VUV Degradation Times and CI Values

Surface degradation of the PVC-MNPs was performed using VUV irradiation exposure times of 0, 30, 45, 60, 75, and 90 min. After degradation, CI values were calculated to assess the oxidative modification of the PVC-MNPs. The CI value was determined using the ratio of the peak height to the C=O stretching band at 1726 cm^{-1} and C-H band at 1426 cm^{-1}, expressed as C=O/C-H. This ratio is considered the degree of degradation [24], which increased with exposure time from 0 to 90 min for each PVC-MNP (Figure 2A–C). Therefore, a correlation analysis was performed to explore the relationship between the degradation time and CI values. As the exposure time increased, the CI values also increased, indicating a strong positive correlation (r = 0.9730, 0.9704, and 0.9473; Figure 2D–F).

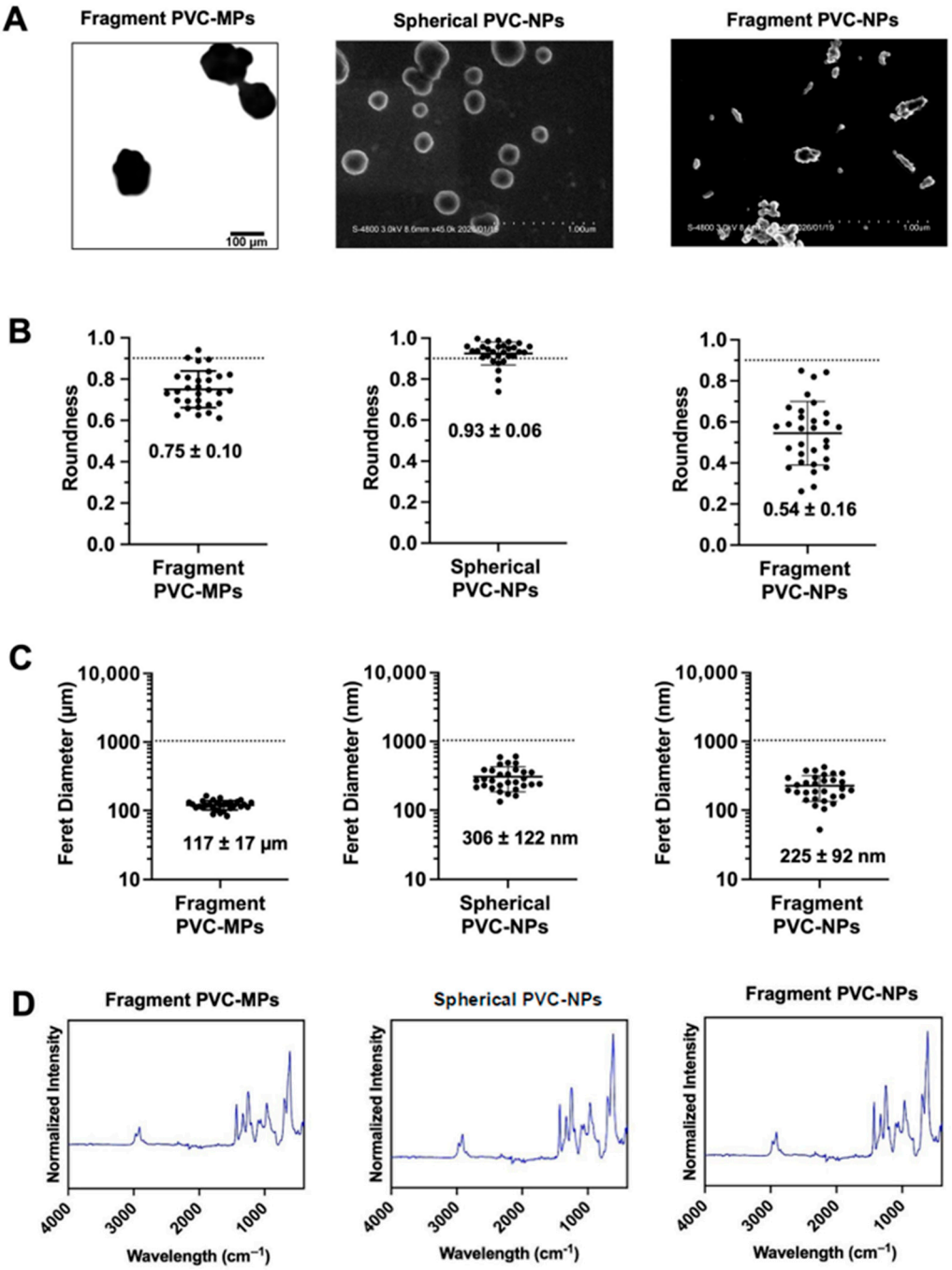

Figure 1. Physicochemical characterization of polyvinyl chloride (PVC-) microplastics and nanoplastics (MNPs). (**A**) Microscopic image of fragmented PVC-microplastics (MPs) (image magnification: 20×, scale bar: 100 µm); scanning electron microscopy (SEM) images of spherical (scale bar: 1 µm) and fragment (scale bar: 1 µm) PVC-MNPs. (**B**,**C**) Roundness and Feret diameter of fragment-shaped PVC-MPs, spherical PVC-NPs, and fragment PVC-nanoplastics (NPs). Analysis was performed based on microscopic and SEM images using ImageJ software (version 2.14.0/1.54f). (**D**) Attenuated Total Reflectance-Fourier Transform Infrared (ATR–FTIR) spectra of fragment PVC–MPs and spherical and fragment PVC–NPs.

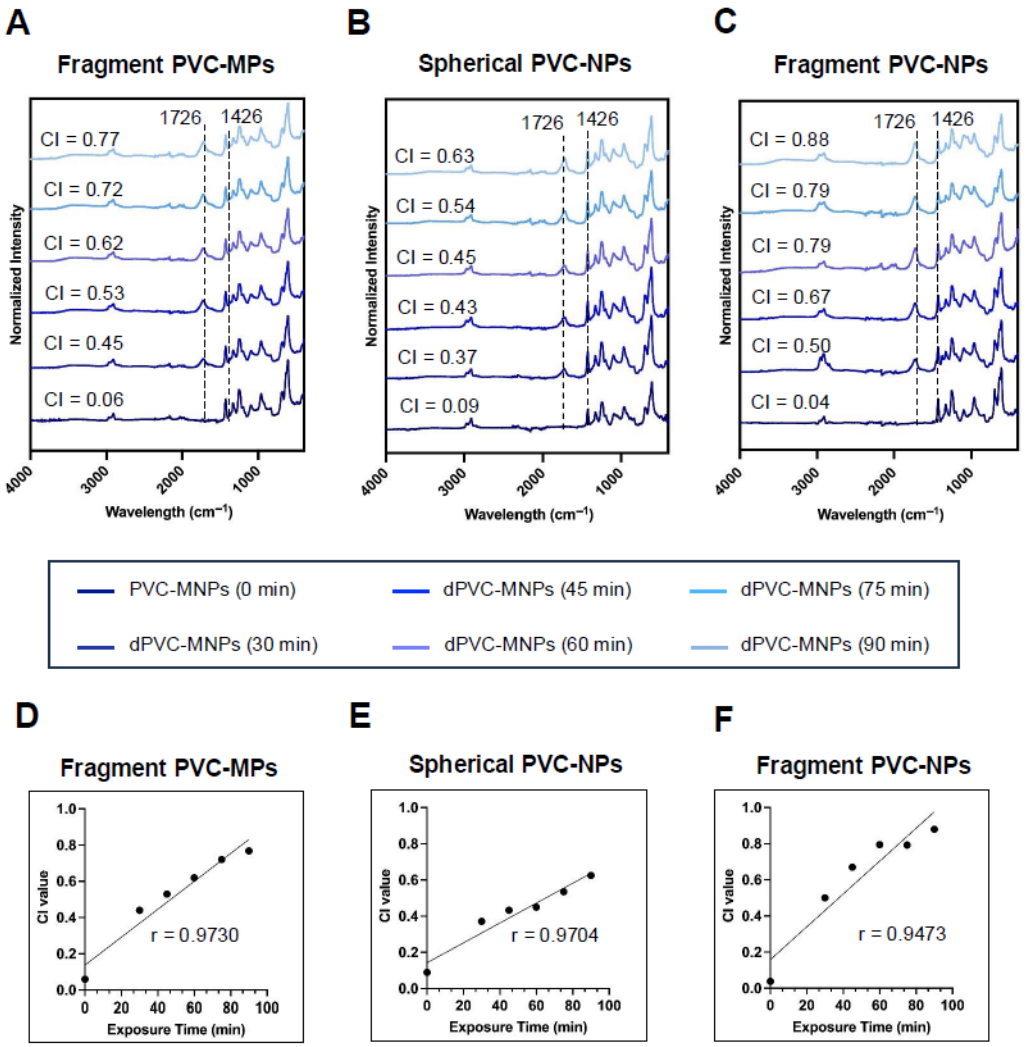

Figure 2. Correlation analysis of vacuum ultraviolet (VUV) degradation times and carbonyl index (CI) values. (**A**) Fragment PVC–MPs, and (**B**) spherical and (**C**) fragment PVC–NPs subjected to VUV degradation for 30, 45, 60, 75, and 90 min, respectively. (**D**–**F**) Correlation analysis evaluating the relationships between degradation time and CI values.

3.3. Cytotoxic Effects of PVC-MNPs

To evaluate the cytotoxicity, A549, Caco-2, and THP-1 cells were used as model cell lines of respiratory, gastrointestinal, and immune system models, respectively. Prior to treatment, degraded PVC-MNPs had undergone three different VUV exposure times (30, 60, and 90 min) with CI values of (0.37 ± 0.03), (0.53 ± 0.06), and (0.66 ± 0.04) for fragment PVC-MPs, (0.27 ± 0.07), (0.46 ± 0.07) and (0.54 ± 0.03) for spherical PVC-NPs, and (0.35 ± 0.06), (0.56 ± 0.08), and (0.68 ± 0.18) for fragment PVC-NPs, respectively. Cells were exposed to non-degraded and degraded PVC-MNPs for 24 h. The concentrations tested were 0.1, 1, 10, and 100 mg/mL for non-degraded and degraded PVC-MPs, and 0.01, 0.1, 1, and 10 mg/mL for non-degraded and degraded PVC-NPs. Degraded fragment PVC-MPs exhibited dose-dependent cytotoxic effects in all cell lines, in contrast to non-degraded ones (Figure 3). Similarly, both degraded spherical and fragment PVC-NPs exhibited dose-dependent cytotoxicity (Spherical PVC-NPs: Figure 4, Fragment PVC-NPs: Figure 5). The quantitative effects of PVC-MNPs were evaluated by calculating the IC_{50} values, where smaller IC_{50} values indicated stronger cytotoxicity (Supplementary Table S1). For the non-degraded PVC-MPs and NPs, the IC_{50} values were greater than 100 and 10 mg/mL, respectively.

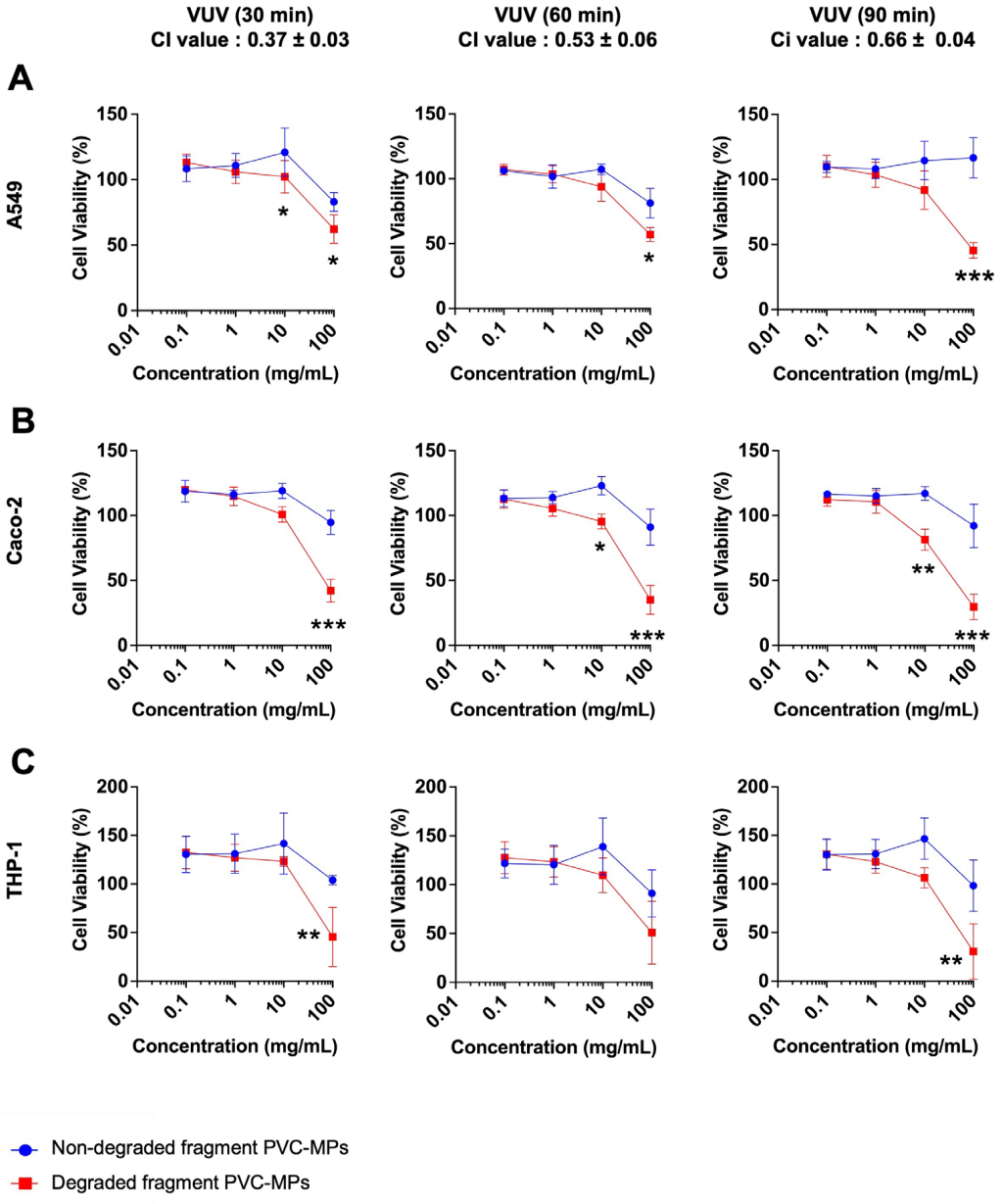

Figure 3. Cytotoxicity of fragment PVC–MPs. (**A**) A549, (**B**) Caco–2, and (**C**) THP–1 cells were seeded into 96–well plates at densities of 1×10^4, 2×10^4, and 2×10^4 cells per well, respectively, and incubated for 24 h. Following incubation, the cells were exposed to non-degraded and VUV–degraded fragment PVC–MPs, with degradation times of 30, 60, and 90 min at various concentrations. After a further 24 h treatment, cell viability was assessed using the MTT assay and IC_{50} value was calculated. Results are presented as mean ± standard deviation (SD) from three independent experiments. Significance was assessed using two–way ANOVA followed by Bonferroni's multiple comparisons test. * $p < 0.05$; ** $p < 0.01$; *** $p < 0.001$.

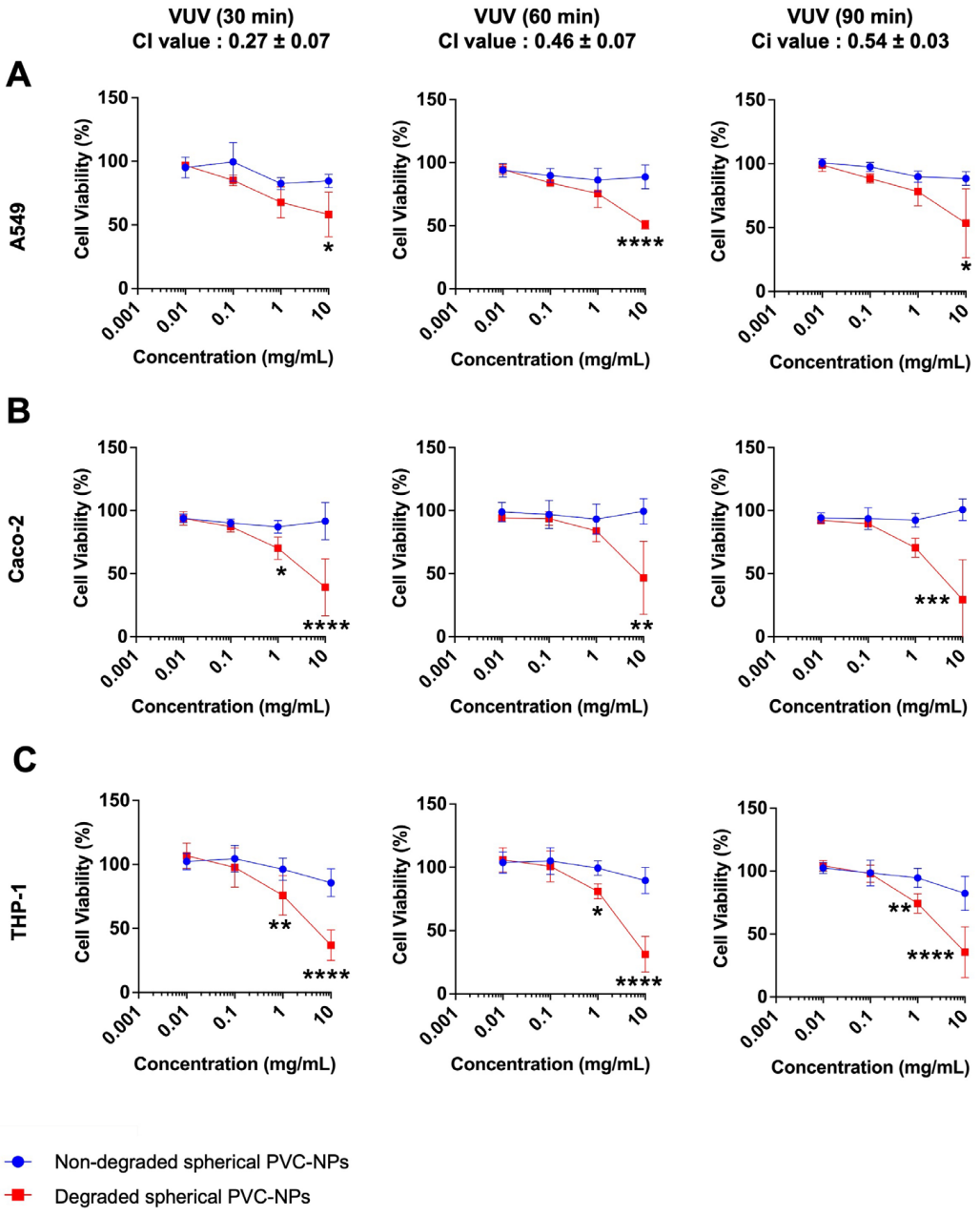

Figure 4. Cytotoxicity of spherical PVC-NPs. (**A**) A549, (**B**) Caco-2, and (**C**) THP-1 cells were seeded into 96–well plates at densities of 1×10^4, 2×10^4, and 2×10^4 cells per well, respectively, and incubated for 24 h. Following incubation, the cells were exposed to non-degraded and VUV-degraded spherical PVC-NPs, with degradation times of 30, 60, and 90 min at various concentrations. After a further 24 h treatment, cell viability was assessed using the MTT assay and IC_{50} value was calculated. Results are presented as mean ± standard deviation (SD) from three independent experiments. Significance was assessed using two–way ANOVA followed by Bonferroni's multiple comparisons test. * $p < 0.05$; ** $p < 0.01$; *** $p < 0.001$; **** $p < 0.0001$.

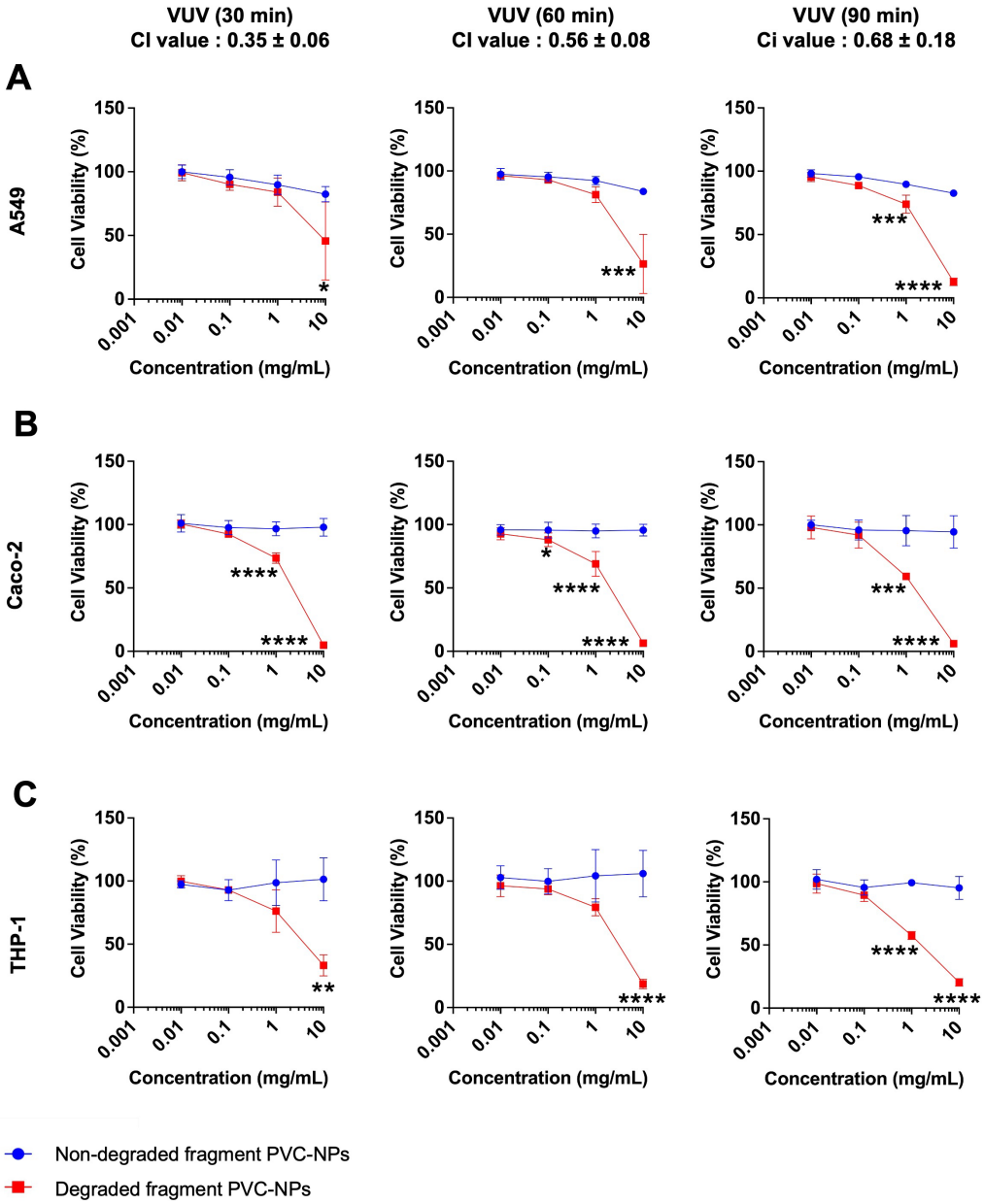

Figure 5. Cytotoxicity of fragment PVC-NPs. (**A**) A549, (**B**) Caco-2, and (**C**) THP-1 cells were seeded into 96–well plates at densities of 1×10^4, 2×10^4, and 2×10^4 cells per well, respectively, and incubated for 24 h. Following incubation, the cells were exposed to non-degraded and VUV-degraded fragment PVC-NPs, with degradation times of 30, 60, and 90 min at various concentrations. After a further 24 h treatment, cell viability was assessed using the MTT assay and IC_{50} value was calculated. Results are presented as mean ± standard deviation (SD) from three independent experiments. Significance was assessed using two–way ANOVA followed by Bonferroni's multiple comparisons test. * $p < 0.05$; ** $p < 0.01$; *** $p < 0.001$; **** $p < 0.0001$.

4. Discussion

This study prepared environmentally relevant PVC-MNPs of varied size and shape, addressing the limited number of studies that have considered the heterogeneous nature of MNPs in the environment [20,22]. MNPs, which reflect environmental samples and are the most commonly encountered polymers, are required for toxicity assessments. Thus, PVC, one of the most commonly found polymers in the environment but with limited use in toxicity studies, was utilized in this study [22]. We synthesized both spherical and fragment PVC-NPs using a precipitation-based method and investigated the influence of

morphological features and size on particle behavior and toxicity. Roundness and Feret diameter measurements confirmed that the produced particles had distinct morphologies, as shown in Figure 1A,B. Furthermore, ATR-FTIR analysis revealed no additional peaks in the PVC-MNP spectra, indicating that the synthesis process did not introduce detectable impurities (Figure 1D), and the prepared PVC-NPs were comparable to commercial polymers in terms of surface chemistry. In this study, spherical PVC-NPs were intentionally included as a reference morphology to explore the effect of shape on particle behavior and toxicity, particularly in comparison to the fragments that dominate real environmental samples.

Considering the surface degradation of MNPs by environmental factors such as ultraviolet (UV) radiation, heat, and humidity is also crucial [31]. MPs in the environment have been reported to exhibit signs of surface degradation with the introduction of oxygen-containing functional groups on the surface of environmental samples, and that the degree of degradation varies among environmental samples [27]. To date, few studies have explored the surface degradation of plastics. Therefore, this study simulated the weathering process using VUV, which introduces the surface degradation of polymers. The VUV-induced surface degradation of the prepared PVC-MNPs was clearly demonstrated by CI analysis, which indicated the formation of oxygen-containing functional groups on the PVC surface (Figure 2A–C). The CI values obtained for the prepared PVC-MNPs were comparable to the CI values reported in a study simulating environmental conditions [31]. Notably, fragment MPs and NPs exhibited relatively higher CI values than spherical NPs in the present study (Figure 2D–F). This difference may be related to the larger surface area or morphological characteristics of the fragment particles, which could promote surface oxidation during the degradation process. A strong positive correlation between degradation time and CI values was also observed (Figure 2D–F), confirming that VUV irradiation induced consistent and measurable, and exposure-/dose-dependent surface oxidation. These findings align with those of previous studies, where PE-MPs exposed to different VUV exposure times at a wavelength of 172 nm induced the formation of a carbonyl group with varied CI values [27] and prolonged exposure increased the CI values [24]. Similarly, other studies have reported that PVC-MPs exposed to UV light from a 1000 W mercury lamp at, 80 W/cm^2 exhibited a new oxygen-containing absorption peak [32], and UV-aged PVC-MPs increased the CI values from 0.003 to 1.02 after 30 days of UV exposure [33]. Notably, PVC exhibited the highest degradation level among plastic polymers owing to its low stability and high sensitivity to sunlight. UV light initiates dechlorination and HCL formation, resulting in an autocatalytic degradation process [31]. These results demonstrate that CI quantification is a reliable indicator of surface weathering and functional group degradation in PVC-MNPs during VUV degradation. Despite clear chemical changes, the absence of morphological alterations suggests that VUV exposure primarily affects the surface chemistry without compromising particle integrity. Additionally, it has been reported that during the environmental weathering process of PVC, various additives can leach from the particles [34,35]. In the present study, we used additive-free PVC-MNPs to focus on the effects of polymer surface degradation itself. However, further studies using additive-containing PVC-MNPs will be necessary to evaluate the potential toxic effects of leached additives under environmentally relevant conditions.

The cytotoxicity of the PVC-MNPs revealed clear distinctions between degraded and non-degraded particles across the tested cell lines (A549, Caco-2, and THP-1). Degraded PVC-MNPs, prepared by VUV exposure for 30, 60, and 90 min, consistently induced dose-dependent cytotoxic effects, whereas their non-degraded counterparts exhibited minimal toxicity. These observations are consistent with those of previous studies, in which VUV-degraded PE-MPs induced significant cytotoxicity in human cell lines compared to non-degraded MNPs [27,28]. The higher cytotoxic effects of degraded PVC-MNPs

may result from the formation of carbonyl (C=O) and hydroxyl (O-H) groups, as well as carboxyl (–COOH) end groups generated during UV-induced chain scission, which collectively increase the hydrophilicity of the particle surface. This enhanced hydrophilicity can improve the particle stability in biological media, thereby increasing the likelihood of cellular interactions, triggering distinct immune responses in macrophage cells, and facilitating cellular uptake through endocytosis [36]. Furthermore, MNPs can trigger both extracellular and intracellular reactive oxygen species (ROS) generation as well as oxidative stress related to the degree of degradation [37,38]. Consequently, ROS overload can damage cellular macromolecules, such as DNA, proteins, and lipids, and impair cellular functions under different MNP exposure conditions. In our previous studies [26,28], PE and PVC MNPs were shown to induce lipid peroxidation accumulation in RAW264.7 cells, suggesting that oxidative stress–mediated lipid peroxidation may represent one possible mechanism underlying MNP-induced cytotoxicity. Although further studies are required to clarify the mechanisms of cell death caused by degraded MNPs, these findings indicate that oxidative damage to cellular components may contribute to the observed cytotoxic effects. However, these effects may differ between MPs and NPs owing to their size-dependent behaviors. Notably, in this study, the degraded PVC-NPs induced stronger cytotoxicity than the degraded PVC-MPs, with lower IC_{50} values. Interestingly, the degraded fragment PVC-NPs and MPs exhibited higher CI values than the degraded spherical PVC-NPs, suggesting that the fragment shape made these particles more susceptible to oxidative modification during VUV exposure (Figure 2A–C). In contrast, the spherical PVC-NPs still induced stronger cytotoxicity than the fragment PVC-MPs, demonstrating that particle size has greater influence on biological responses than oxidation level alone. Nevertheless, their high specific surface area and greater likelihood of cellular uptake also enhance the ability of NPs to interact with cells. Overall, the cytotoxicity pattern reflects the combined influence of particle shape, size, and surface oxidation.

While the concentrations applied in this study are higher than those typically detected in the environment, these levels were intentionally chosen to reflect the possibility of intracellular accumulation of MNPs over time and to investigate the threshold at which adverse cellular effects may emerge. Therefore, a wide range of concentrations was tested in order to identify the level at which cytotoxic effects could be detected. At such high concentrations, additional factors such as hypoxia, sedimentation-related stress, or physical interactions between particles and cells may also contribute to the observed cytotoxicity.

5. Conclusions

This study provides valuable insights into the physicochemical characteristics of MNPs, such as their size, shape, and surface degradation, as well as their potential cytotoxic effects on various cell lines. In fact, further research, particularly biological assessments using environmentally relevant concentrations as well as the degraded states of MNPs from different polymer types, is needed to deepen our understanding. More importantly, as environmental MNPs contain plastic additives, a systematic and comprehensive cytotoxic assessment of these additives and the associated health risks of plastic exposure is urgently required.

Supplementary Materials: The following supporting information can be downloaded at: https://www.mdpi.com/article/10.3390/microplastics5020083/s1, Supplementary Table S1: IC_{50} values of PVC-MNPs.

Author Contributions: Conceptualization, Y.H.; data curation, P.B.B.A.; visualization, P.B.B.A.; validation, P.B.B.A., S.M., W.I., M.H., Y.M., and A.M.; writing—original draft preparation, P.B.B.A. and Y.H.; writing—review and editing, P.B.B.A., Y.H., S.M., W.I., M.H., Y.M., A.M., K.H., and Y.T.;

supervision, K.H., Y.H. and Y.T.; project administration, Y.H. and Y.T.; funding acquisition, Y.H., Y.T. All authors have read and agreed to the published version of the manuscript.

Funding: This work was supported by the Environment Research and Technology Development Fund (JPMEERF20241003) of the Environmental Restoration and Conservation Agency provided by the Ministry of the Environment of Japan, Japan Society for the Promotion of Science (Grant Number 21K19336, 25K20572), Fuji Seal Foundation, Steel Foundation for Environmental Protection Technology and Sumitomo Foundation for Environmental Research Projects. This research was partially supported by the Research Support Project for Life Science and Drug Discovery (Basis for Supporting Innovative Drug Discovery and Life Science Research) from AMED under Grant Number JP25ama121054.

Institutional Review Board Statement: Not applicable.

Informed Consent Statement: Not applicable.

Data Availability Statement: All data analyzed in this study are included in the manuscript or Supplementary Information Files. Further inquiries can be directed to the corresponding authors.

Acknowledgments: This research was partially supported by the Research Support Project for Life Science and Drug Discovery (Basis for Supporting Innovative Drug Discovery and Life Science Research) from AMED under Grant Number JP25ama121054. SEM analysis was supported by Center for Medical Research and Education (CentMeRE), Graduate School of Medicine, The University of Osaka.

Conflicts of Interest: The authors declare no conflicts of interest.

References

1. Li, Y.; Tao, L.; Wang, Q.; Wang, F.; Li, G.; Song, M. Potential Health Impact of Microplastics: A Review of Environmental Distribution, Human Exposure, and Toxic Effects. *Environ. Health* **2023**, *1*, 249–257. [CrossRef] [PubMed]
2. Kannan, K.; Vimalkumar, K. A Review of Human Exposure to Microplastics and Insights Into Microplastics as Obesogens. *Front. Endocrinol.* **2021**, *12*, 724989. [CrossRef] [PubMed]
3. OECD. *Global Plastics Outlook: Policy Scenarios to 2060*; OECD: Paris, France, 2022; ISBN 978-92-64-97364-0.
4. Thompson, R.C.; Olsen, Y.; Mitchell, R.P.; Davis, A.; Rowland, S.J.; John, A.W.G.; McGonigle, D.; Russell, A.E. Lost at Sea: Where Is All the Plastic? *Science* **2004**, *304*, 838. [CrossRef] [PubMed]
5. Estahbanati, S.; Upadhyaya, G.; Wells, M.J.M.; Bell, K.Y. Primary and Secondary Microplastic and Nanoplastic Regulations: Perspectives on Water Industry Impacts. *J. Environ. Prot.* **2024**, *15*, 697–715. [CrossRef]
6. Osman, A.I.; Hosny, M.; Eltaweil, A.S.; Omar, S.; Elgarahy, A.M.; Farghali, M.; Yap, P.-S.; Wu, Y.-S.; Nagandran, S.; Batumalaie, K.; et al. Microplastic Sources, Formation, Toxicity and Remediation: A Review. *Environ. Chem. Lett.* **2023**, *21*, 2129–2169. [CrossRef]
7. Valsesia, A.; Parot, J.; Ponti, J.; Mehn, D.; Marino, R.; Melillo, D.; Muramoto, S.; Verkouteren, M.; Hackley, V.A.; Colpo, P. Detection, Counting and Characterization of Nanoplastics in Marine Bioindicators: A Proof of Principle Study. *Microplastics Nanoplastics* **2021**, *1*, 5. [CrossRef]
8. Kochanek, A.; Grąz, K.; Potok, H.; Gronba-Chyła, A.; Kwaśny, J.; Wiewiórska, I.; Ciuła, J.; Basta, E.; Łapiński, J. Micro- and Nanoplastics in the Environment: Current State of Research, Sources of Origin, Health Risks, and Regulations—A Comprehensive Review. *Toxics* **2025**, *13*, 564. [CrossRef]
9. Thompson, R.C.; Courtene-Jones, W.; Boucher, J.; Pahl, S.; Raubenheimer, K.; Koelmans, A.A. Twenty Years of Microplastic Pollution Research—What Have We Learned? *Science* **2024**, *386*, eadl2746. [CrossRef]
10. Sangkham, S.; Faikhaw, O.; Munkong, N.; Sakunkoo, P.; Arunlertaree, C.; Chavali, M.; Mousazadeh, M.; Tiwari, A. A Review on Microplastics and Nanoplastics in the Environment: Their Occurrence, Exposure Routes, Toxic Studies, and Potential Effects on Human Health. *Mar. Pollut. Bull.* **2022**, *181*, 113832. [CrossRef]
11. Nihart, A.J.; Garcia, M.A.; El Hayek, E.; Liu, R.; Olewine, M.; Kingston, J.D.; Castillo, E.F.; Gullapalli, R.R.; Howard, T.; Bleske, B.; et al. Bioaccumulation of Microplastics in Decedent Human Brains. *Nat. Med.* **2025**, *31*, 1114–1119. [CrossRef]
12. Prattichizzo, F.; Ceriello, A.; Pellegrini, V.; La Grotta, R.; Graciotti, L.; Olivieri, F.; Paolisso, P.; D'Agostino, B.; Iovino, P.; Balestrieri, M.L.; et al. Micro-Nanoplastics and Cardiovascular Diseases: Evidence and Perspectives. *Eur. Heart J.* **2024**, *45*, 4099–4110. [CrossRef]
13. Yang, Y.; Xie, E.; Du, Z.; Peng, Z.; Han, Z.; Li, L.; Zhao, R.; Qin, Y.; Xue, M.; Li, F.; et al. Detection of Various Microplastics in Patients Undergoing Cardiac Surgery. *Environ. Sci. Technol.* **2023**, *57*, 10911–10918. [CrossRef]

14. Wick, P.; Malek, A.; Manser, P.; Meili, D.; Maeder-Althaus, X.; Diener, L.; Diener, P.-A.; Zisch, A.; Krug, H.F.; Von Mandach, U. Barrier Capacity of Human Placenta for Nanosized Materials. *Environ. Health Perspect.* **2010**, *118*, 432–436. [CrossRef] [PubMed]
15. Saraluck, A.; Techarang, T.; Bunyapipat, P.; Boonchuwong, K.; Pullaput, Y.; Mordmuang, A. Detection of Microplastics in Human Breast Milk and Its Association with Changes in Human Milk Bacterial Microbiota. *J. Clin. Med.* **2024**, *13*, 4029. [CrossRef]
16. Brits, M.; Van Velzen, M.J.M.; Sefiloglu, F.Ö.; Scibetta, L.; Groenewoud, Q.; Garcia-Vallejo, J.J.; Vethaak, A.D.; Brandsma, S.H.; Lamoree, M.H. Quantitation of Micro and Nanoplastics in Human Blood by Pyrolysis-Gas Chromatography–Mass Spectrometry. *Microplastics Nanoplastics* **2024**, *4*, 12. [CrossRef]
17. Yan, Z.; Liu, Y.; Zhang, T.; Zhang, F.; Ren, H.; Zhang, Y. Analysis of Microplastics in Human Feces Reveals a Correlation between Fecal Microplastics and Inflammatory Bowel Disease Status. *Environ. Sci. Technol.* **2022**, *56*, 414–421. [CrossRef] [PubMed]
18. Zhao, B.; Rehati, P.; Yang, Z.; Cai, Z.; Guo, C.; Li, Y. The Potential Toxicity of Microplastics on Human Health. *Sci. Total Environ.* **2024**, *912*, 168946. [CrossRef]
19. Marfella, R.; Prattichizzo, F.; Sardu, C.; Fulgenzi, G.; Graciotti, L.; Spadoni, T.; D'Onofrio, N.; Scisciola, L.; La Grotta, R.; Frigé, C.; et al. Microplastics and Nanoplastics in Atheromas and Cardiovascular Events. *N. Engl. J. Med.* **2024**, *390*, 900–910. [CrossRef] [PubMed]
20. Lim, X. Microplastics Are Everywhere—But Are They Harmful? *Nature* **2021**, *593*, 22–25. [CrossRef]
21. Egbuna, C.; Parmar, V.K.; Jeevanandam, J.; Ezzat, S.M.; Patrick-Iwuanyanwu, K.C.; Adetunji, C.O.; Khan, J.; Onyeike, E.N.; Uche, C.Z.; Akram, M.; et al. Toxicity of Nanoparticles in Biomedical Application: Nanotoxicology. *J. Toxicol.* **2021**, *2021*, 1–21. [CrossRef]
22. Pelegrini, K.; Pereira, T.C.B.; Maraschin, T.G.; Teodoro, L.D.S.; Basso, N.R.D.S.; De Galland, G.L.B.; Ligabue, R.A.; Bogo, M.R. Micro- and Nanoplastic Toxicity: A Review on Size, Type, Source, and Test-Organism Implications. *Sci. Total Environ.* **2023**, *878*, 162954. [CrossRef]
23. Alavian Petroody, S.S.; Hashemi, S.H.; Škrlep, L.; Mušič, B.; Van Gestel, C.A.M.; Sever Škapin, A. UV Light Causes Structural Changes in Microplastics Exposed in Bio-Solids. *Polymers* **2023**, *15*, 4322. [CrossRef]
24. Ikuno, Y.; Tsujino, H.; Haga, Y.; Asahara, H.; Higashisaka, K.; Tsutsumi, Y. Impact of Degradation of Polyethylene Particles on Their Cytotoxicity. *Microplastics* **2023**, *2*, 192–201. [CrossRef]
25. Chen, B.; He, B.; Wu, H.; Liu, A. Microplastic Degradations in Simulated UV Light, Natural Light and Natural Water Body: A Comparison Investigation. *Emerg. Contam.* **2024**, *10*, 100306. [CrossRef]
26. Manabe, S.; Haga, Y.; Tsujino, H.; Ikuno, Y.; Asahara, H.; Higashisaka, K.; Tsutsumi, Y. Treatment of Polyethylene Microplastics Degraded by Ultraviolet Light Irradiation Causes Lysosome-Deregulated Cell Death. *Sci. Rep.* **2024**, *14*, 24008. [CrossRef]
27. Ikuno, Y.; Tsujino, H.; Haga, Y.; Manabe, S.; Idehara, W.; Hokaku, M.; Asahara, H.; Higashisaka, K.; Tsutsumi, Y. Polyethylene, Whose Surface Has Been Modified by UV Irradiation, Induces Cytotoxicity: A Comparison with Microplastics Found in Beaches. *Ecotoxicol. Environ. Saf.* **2024**, *277*, 116346. [CrossRef] [PubMed]
28. Manabe, S.; Haga, Y.; Tsujino, H.; Ikuno, Y.; Idehara, W.; Hokaku, M.; Bo Bo Aung, P.; Asahara, H.; Higashisaka, K.; Tsutsumi, Y. Vacuum Ultraviolet-Induced Degradation of Polyethylene and Polyvinyl Chloride Micro/Nanoplastics Enhances Their Cytotoxicity and Lipid Peroxidation Level. *Ecotoxicol. Environ. Saf.* **2025**, *303*, 119030. [CrossRef]
29. Tanaka, K.; Takahashi, Y.; Kuramochi, H.; Osako, M.; Tanaka, S.; Suzuki, G. Preparation of Nanoscale Particles of Five Major Polymers as Potential Standards for the Study of Nanoplastics. *Small* **2021**, *17*, 2105781. [CrossRef]
30. Lee, W.S.; Kim, H.; Sim, Y.; Kang, T.; Jeong, J. Fluorescent Polypropylene Nanoplastics for Studying Uptake, Biodistribution, and Excretion in Zebrafish Embryos. *ACS Omega* **2022**, *7*, 2467–2473. [CrossRef]
31. Maddison, C.; Sathish, C.I.; Lakshmi, D.; Wayne, O.; Palanisami, T. An Advanced Analytical Approach to Assess the Long-Term Degradation of Microplastics in the Marine Environment. *Npj Mater. Degrad.* **2023**, *7*, 59. [CrossRef]
32. Liu, Z.; Tao, R.; Li, H.; Qu, M.; Hu, C.; Mei, Y. Impact of the Aged Polyvinyl Chloride Microplastics on the Adsorption Behavior of Tildipirosin and Environmental Risk Assessment. *Water Air Soil. Pollut.* **2025**, *236*, 194. [CrossRef]
33. Tumrani, S.H.; Sharma, B.P.; Soomro, R.A.; Mersal, G.A.M.; Fallatah, A.M.; Ibrahim, M.M.; Karakuş, S. UV-driven Surface Oxidation of PVC Microplastics and Their Interaction with Emerging Pollutants. *Colloid Polym. Sci.* **2025**, *303*, 2129–2141. [CrossRef]
34. Simon, M.; Hartmann, N.; Vollertsen, J. Accelerated Weathering Increases the Release of Toxic Leachates from Microplastic Particles as Demonstrated through Altered Toxicity to the Green Algae Raphidocelis Subcapitata. *Toxics* **2021**, *9*, 185. [CrossRef]
35. Gao, L.; Su, Y.; Mehmood, T.; Wang, Z.; Peng, L.; Zhang, N. UVA-Induced Weathering of Microplastics in Seawater: Surface Property Transformations and Kinetics. *Front. Mar. Sci.* **2025**, *12*, 1519668. [CrossRef]
36. Desai, D.; Åkerfelt, M.; Prabhakar, N.; Toriseva, M.; Näreoja, T.; Zhang, J.; Nees, M.; Rosenholm, J.M. Factors Affecting Intracellular Delivery and Release of Hydrophilic Versus Hydrophobic Cargo from Mesoporous Silica Nanoparticles on 2D and 3D Cell Cultures. *Pharmaceutics* **2018**, *10*, 237. [CrossRef] [PubMed]

37. Jeon, S.; Lee, D.-K.; Jeong, J.; Yang, S.I.; Kim, J.-S.; Kim, J.; Cho, W.-S. The Reactive Oxygen Species as Pathogenic Factors of Fragmented Microplastics to Macrophages. *Environ. Pollut.* **2021**, *281*, 117006. [CrossRef]
38. Mahmud, F.; Sarker, D.B.; Jocelyn, J.A.; Sang, Q.-X.A. Molecular and Cellular Effects of Microplastics and Nanoplastics: Focus on Inflammation and Senescence. *Cells* **2024**, *13*, 1788. [CrossRef]